BMC Ophthalmology

RESEARCH

Open Access

# Do the monocyte-derived dendritic cells exert a pivotal role in the early onset of experimental autoimmune uveitis?

Bo Yuan[1,4†], Yajie Wang[2,3†], Yanhua Chu[2,3] and Xiaoyong Yuan[1,2,3*]

## Abstract

**Background** Eyes are recognized as immunological privileged site. However, the onset of autoimmune uveitis (AU) prompts an influx of dendritic cells (DCs) into the retinas, tasked with presenting auto-antigens, thereby exacerbating the inflammatory response. Monocyte-derived DCs (moDCs) implicated in various autoimmune disorders, but their specific involvement in AU remains unclear. This study aims to investigate the constitution and dynamics of retinal DCs subsequent to the induction of experimental autoimmune uveitis (EAU).

**Methods** In our study, an EAU model was established in C57BL/6J mice, and prednisolone acetate (PA) eye drops were administrated unilaterally to the right eye from 5 days post-immunization (dpi). The infiltration of Gr-1$^{+}$CD115$^{+}$CD11c$^{-}$MHC-II$^{-}$ cells (monocytes), Gr-1$^{+}$CD115$^{+}$CD11c$^{+}$MHC-II$^{+}$ cells (moDCs) and Gr-1$^{-}$CD115$^{-}$CD11c$^{+}$MHC-II$^{+}$ cells (conventional dendritic cells, cDCs) within retina were detected by flow cytometry and immunofluorescence stain at 7, 10, 13, and 16 dpi. Additionally, the protein expression and mRNA expression of pivotal cytokines associated with moDCs and inflammation were analysed by western blotting and quantitative real-time polymerase chain reaction (qRT-PCR), respectively.

**Results** Our findings unveiled a notable rise in moDCs infiltration and differentiation from 7 to 13 dpi. The administration of PA eye drops did not yield a significant variance in either the quantity or the differentiation rate of moDCs. Throughout the initial stages of EAU, the expression of GM-CSF remained consistent, while TGF-β1 exhibited a sustained increase until 13 dpi in the control group and until 10 dpi following PA treatment. Anti-inflammatory cytokines *Il-10* and *Il-4* displayed no significant increase until 16 dpi after PA administration.

**Conclusions** Our results indicate that moDCs exhibited an earlier and more substantial infiltration into the inflamed retina compared to cDCs. This heightened presence of moDCs appeared to play a dominant role in the presentation of auto-antigens during the initial stages of EAU, consequently contributing to the exaggerated autoimmune response within the ocular milieu. The administration of PA exhibited no discernible impact on either the differentiation or the infiltration of moDCs.

†Bo Yuan and Yajie Wang these authors contributed equally to this work.

*Correspondence:
Xiaoyong Yuan
yuanxy_cn@hotmail.com

Full list of author information is available at the end of the article

**Keywords** Autoimmune disorder, Uveitis, Dendritic cell, Monocyte-derived dendritic cell, Corticosteroids

## Background

Uveitis is a multifaceted and potentially severe ocular condition characterized by inflammation within the uvea, which progressively leads to a spectrum of complications, including cataracts, glaucoma, macular edema, and in severe cases, irreversible vision loss, but the pathogenesis of uveitis has remained elusive [1]. Autoimmune uveitis (AU) predominantly affects individuals in the middle-aged population, with reported rates of vision impairment ranging from 5 to 25% [2]. In recent years, noteworthy-increasing evidence underscored the etiological relationship between AU and systemic autoimmune disorders [3]. Given the distinctive immune-privileged microenvironment of ocular tissues, it is imperative to figure out the crucial immune cells and cytokines involved in uveitis for the development of precise and comprehensive therapeutic approaches.

Ocular immune privilege is a crucial mechanism ensuring a high-preserved environment essential for maintaining normal vision. This privilege is upheld through diverse mechanisms, including the integrity of the blood-retina barrier (BRB), the absence of lymphatic drainage, and the abundance of anti-inflammatory cells and cytokines [4]. Among the immune cells involved, dendritic cells (DCs) stand as the most specialized antigen-presenting cells (APCs), orchestrating pivotal roles in initiating and regulating adaptive immune responses and promoting tolerance to self-antigens [5]. Previous researches have suggested that when the anti-inflammatory environment is disrupted, migrated DCs tend to exacerbate the pathophysiology of autoimmune diseases, contrasting with the tendency of resident ocular DCs to display a tolerogenic phenotype [6]. However, due to the lack of lymphatic drainage, the migration of conventional DCs (cDCs) are supposed to be restricted within the ocular tissues. Consequently, the origin of migrated DCs responsible for the early stages of AU remains unclear.

In inflammatory environments, monocytes are recruited and differentiate into DCs expressing major histocompatibility complex (MHC) molecules under the influence of cytokines especially granulocyte-macrophage colony-stimulating factor (GM-CSF) and transforming growth factor beta (TGF-β), These differentiated cells, known as monocyte-derived DCs (moDCs) or inflammatory DCs [7], have been identified in various inflammation-relative diseases [8], including rheumatoid arthritis [9], multiple sclerosis [10, 11], lupus nephritis [12], allergic rhinitis [13], as well as various murine models of autoimmune diseases, such as antigen-induced arthritis, collagen-induced arthritis, dextran sulfate sodium-induced colitis [14] and experimental autoimmune encephalomyelitis [15]. Functionally similar to monocytes, moDCs possess the capability to produce diverse inflammatory cytokines and chemokines [16, 17], maintain interactions with other cells [18], and consequently amplifying the inflammatory response during autoimmune disorders.

In the pathogenesis of uveitis, the migration of $CD4^+$ T cells toward the retina initiates an immune response, leading to subsequent damage to retinal pigment epithelial (RPE) cells and activation of vascular endothelial cells [19]. These activated cells release significant quantities of GM-CSF, TGF-β, and other inflammatory cytokines [20], potentially fostering an environment conducive to the differentiation of moDCs and exacerbating the ocular autoimmune response.

The murine model of EAU is a widely utilized experimental model for investigating the underlying mechanisms and potential therapeutic approaches for uveitis [21, 22]. EAU effectively replicates several aspects of human uveitis by eliciting an inflammatory response in ocular tissues through subcutaneous administration of ocular antigens in combination with adjuvants. Around 7 days after immunization, immune response activation leads to the recruitment and infiltration of immune cells into ocular tissues, resulting in moderate to severe damage to the uvea and retina [23]. EAU mouse model offers a valuable tool for studying the cellular and molecular mechanisms implicated in uveitis.

In our research, we induced EAU in C57BL/6J mice and examined the dynamics and distribution of retinal monocytes, moDCs, and cDCs, alongside the expression of key cytokines involved in DC differentiation and the inflammatory response at 7, 10, 13, and 16 dpi. Our findings, for the first time, unveiled an escalating trend of moDC infiltration and an earlier presence of moDCs compared to cDCs during EAU progression. Additionally, we observed that glucocorticoid eye drop failed to hinder the infiltration and differentiation of moDC in retina. These observations suggest the predominant involvement of moDCs, rather than cDCs, in the initial stages of EAU, which reinforces the significance of exploring novel therapeutic strategies specifically targeting moDCs for uveitis treatment.

## Materials and methods

### Animal experiment

Six- to eight-week-old female C57BL/6J mice were obtained from Beijing Vital River Laboratory Animal Technology Co., Ltd. (Beijing, China) and housed under specific pathogen-free conditions following standardized procedures. EAU was inducted by subcutaneous

injection of a uveitogenic peptide [21] after anesthesia with intraperitoneal injection of 1.25% tribromoethyl aicolaol (200 μL/10 g, Avertin, Aibei Biotechnology Co., Ltd., Nanjing, Jiangsu, China). Briefly, a 1:1 v/v emulsion containing 200 μg $hIRBP_{651\text{-}670}$ (LAQGAYRTAVDLES-LASQLT) and complete Freund's adjuvant containing 2.5 mg/mL *Mycobacterium* tuberculosis H37RA (Chondrex Inc., Woodinville, WA, USA) were administered via subcutaneous injection 30 min later following an intraperitoneal injection of pertussis toxin (PTX, Sigma-Aldrich Corp., St. Louis, MO, USA). The right eyes of EAU mice were topically treated once a day with 0.01% PA eye drop (PredForte, Allergan Inc., North Chicago, Illinois, USA) from 5 dpi until sacrifice. Protocols for all animal procedures were approved by the Nankai University Animal Care and Use Committee and complied with National Institutes of Health (NIH) guidelines.

### Flow cytometry

The eyes were enucleated at 7, 10, 13, 16 dpi from EAU mice for retinal cell collection, respectively. After dissecting the retina, single-cell suspension was prepared by grinding on a 70-μm cell strainer. Fluorescent antibodies of (PE)-conjugated Gr-1 (Ly-6 C/Ly-6G, Clone RB6-8C5), (PE-Cy7)-conjugated CD11c (Clone N418) from Bio-Lenged (San Diego, CA, USA), (APC)-conjugated MHC Class II (Clone M5/114.15.2) from Proteintech Group, Inc. (Wuhan, Hubei, China), mouse monoclonal primary antibody of α-CD115 from Santa Cruz Biotechnology Inc. (Dallas, TX, USA) and secondary detection goat anti-mouse IgG1 Alexa™ 488 were used to stain retinal single-cell suspensions, according to the manufacturer's protocol for the corresponding antibodies. Subsequently, each sample was analyzed using LSR Fortessa (BD Biosciences, CA, USA) with 100,000 events were collected and the data were analysed by FlowJo™ software (Tree Star, Ashland, OR, USA).

### Immunofluorescence staining

After euthanized by cervical dislocation, eyes were enucleated at 7, 10, 13 and 16 dpi and fixed in 4% PFA (paraformaldehyde) at room temperature. Retinas were dissected and prepared as flattened whole mounts by making 4 radial cuts. Whole-mounted immunofluorescence was performed with mouse monoclonal α-CD115 primary antibody (1:200; Santa Cruz Biotechnology Inc.,

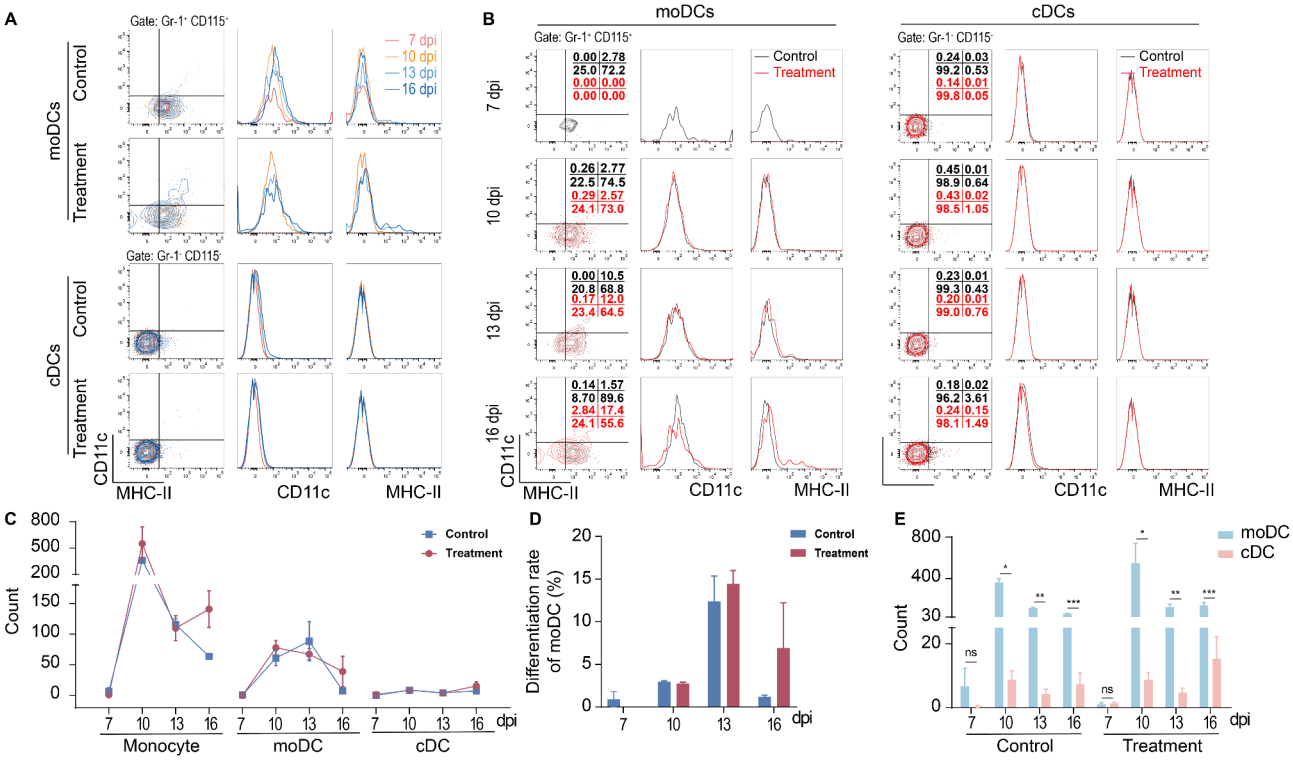


**Fig. 1** The dynamics of monocytes, moDCs and cDCs in the retinas of EAU. (**A** & **B**) The expression of CD11c and MHC-II on Gr-1 + CD115 + CD11c + MHC-II + cells (**A**) and Gr-1-CD115-CD11c + MHC-II + cells (**B**). Numbers represent percentage of cells from the single cells. (**C**) The percentage of monocytes, moDCs, cDCs in the remained cells excluding retinal parenchymal cells from 7 to 16 dpi of EAU. (**D**) The comparation of the percentage of moDCs and cDCs. (**E**) The percentage of moDCs in monocyte indicating the differentiation rate of moDCs. $n = 3$ biologically independent experiments. Data in C were compared using one-way ANOVA, and showed there was no significant difference among each time point. Data in **D** and **E** were analyzed via unpaired *t* test. ns, no significance; $^{*}p < 0.05$, $^{**}p < 0.01$

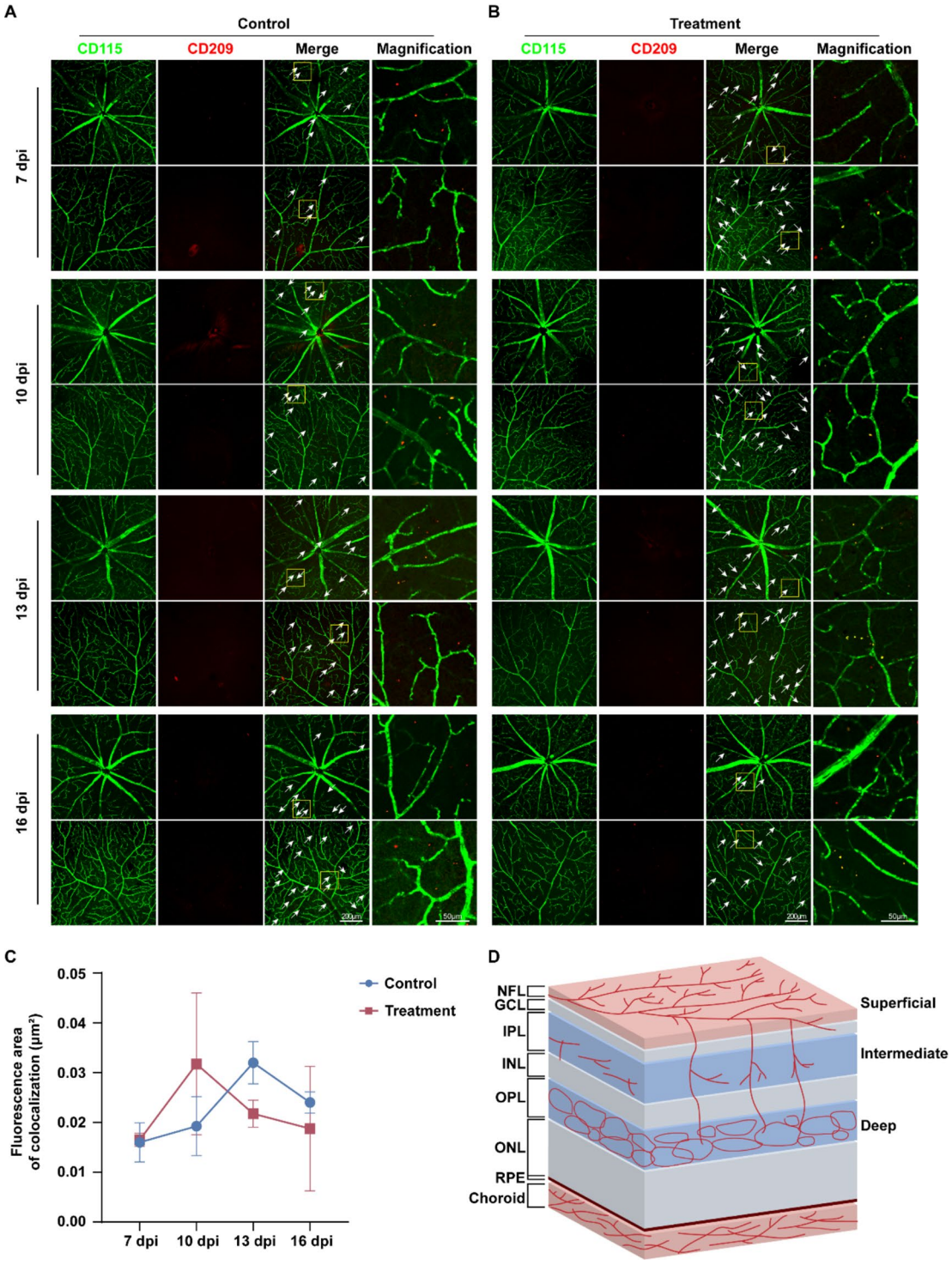


**Fig. 2** Distribution of moDCs in retinas of mice with EAU. (**A** & **B**) CD115 (green), CD209 (red) and both signals in superficial plexuses from central and peripheral retinas of mice with EAU at different time points with (**B**) or without (**A**) PA eye drop treatment. Arrows indicate the co-localizations of CD115 and CD209. The rightmost row is magnifications from the regions framed in yellow. (**C**) Statistical analysis of the co-localization of CD115- and CD209-positive areas in retina respectively between the control and treatment group ($n=4$ biologically independent experiments, one-way ANOVA). (**D**) Schematic diagram depicting the retinal layers and the position of each vascular plexus. NFL: nerve fiber layer, GCL: ganglion cell layer, IPL: inner plexiform layer, INL: inner nuclear layer, OPL: outer plexiform layer, ONL: outer nuclear layer, RPE: retinal pigment epithelial. 200 µm and 50 µm scale bars are for photomontages and magnifications, respectively

Dallas, TX, USA) and rabbit α-CD209 (1:100; Company ABclonal Inc.). Secondary detection was carried out with goat α-mouse IgG1 Alexa™ 488 and Donkey α-rabbit Alexa™ 647 IgG (H + L) secondary antibodies (1:500; Thermo Fisher Scientific Inc., Waltham, Massachusetts, USA).

#### Western blot analysis

Murine retinas were harvested and homogenized in ice-cold Radio immunoprecipitation assay (RIPA) lysis buffer containing 50 mM Tris-HCl (pH 7.4), 150 mM NaCl, and 1% Triton X-100, 1% sodium deoxycholate and 0.1% sodium dodecyl sulfate (SDS), with a protease inhibitor cocktail. Each protein sample (15 μg) was separated by SDS-polyacrylamide gel electrophoresis (SDS-PAGE) for GM-CSF and TGF-β1 respectively, and then transferred onto polyvinylidene difluoride (PVDF) membranes. After blocking with Protein Free Rapid Blocking Buffer (Epizyme Biomedical Technology Co., Ltd., Shanghai, China), immunoblots were incubated overnight at 4℃ with rabbit anti-mouse GM-CSF and rabbit anti-mouse TGF-β1 polyclonal primary antibodies (1:4000 and 1:3000 respectively; Company ABclonal Inc., Wuhan, Hubei, China). Following incubation with the appropriate secondary antibody, the immunoreactive bands were visualized using Tanon 5200 Multi Automatic Chemiluminescence Fluorescence Imaging Analysis System (Tanon, Shanghai, China) and quantified with a loading control of β-actin.

#### Measurement of cytokine expression

Retinal mRNA was extracted at 7, 10, 13, and 16 dpi using TRIzol reagent (Life Technologies, Carlsbad, California, USA) and the reverse transcription of the RNA to complementary DNA (cDNA) via TransScript First-Strand cDNA Synthesis SuperMix (TransGen Biotech, Beijing, China) according to the manufacturer's protocols. mRNA expression was measured by quantitative real-time polymerase chain reaction (qRT-PCR) using Hieff™ qPCR SYBR Green Master Mix (Yeasen Biotechnology Co., Ltd., Shanghai, China) with *β-actin* as the internal control in a CFX96 Touch Real-Time PCR Detection System (Bio-Rad Laboratories, Inc., Hercules, California, USA). The relative gene expression levels were calculated based on the comparative $2^{-\Delta\Delta Ct}$ method. All procedures were repeated in triplicate. Primer sequences are listed in Supplementary Table 1.

#### Confocal microscopy and image analysis

Immunofluorescence images were captured with a TCS SP8 confocal microscope (Leica Camera AG, Berlin, Germany). The conversion of images to 8-bit grayscale prior to thresholding was manipulated by ImageJ software (1.53t, NIH, http://imagej.nih.gov/ij) and subsequently calculated the positive areas of colocalization fluorescence of CD115 and CD209 immunostaining.

#### Statistical analysis

All results are presented as mean ± standard error (SEM) with the indicated sample size and analysed via GraphPad Prism 8 software (GraphPad, San Diego, CA, USA). Biological replicates were used in all experiments. Unpaired *t*-test was used to analyse the statistical significance between control and treatment groups at each time point, as well as that between the amount of moDCs and cDCs. One-way analysis of variance (ANOVA) was used to analyse the statistical significance among multiple groups. The significance threshold was $p$-value $< 0.05$.

## Results

#### MoDCs infiltrated earlier than cDCs in the retina of EAU mice with a higher amount

In general, the disease progression of EAU can be divided into four distinct stages. Following immunization, EAU mice typically manifest initial signs characterized by mild inflammation between days 10 and 14. Subsequent intensification of the inflammatory response occurs between days 14 and 18, marked by protein exudation and fibrin deposition. A progression to retinal vasculitis and edema transpires between days 18 and 24. Beyond the initial 24-day period, the inflammatory reaction gradually diminishes, signalling the onset of the recovery phase [24].

To investigate the dynamics of monocytes, moDCs, and cDCs in the inflamed retina from the early stage through the disease onset, flow cytometry analysis was performed at 7, 10, 13, and 16 dpi. Gating strategies were employed, excluding most retinal parenchymal cells based on their FSC-$A^{lo}$ and SSC-$A^{lo}$ profiles. The remaining cells were further characterized using markers Gr-1, CD115, CD11c, and MHC-II. Gr-$1^+$$CD115^+$ cells identified monocyte-derived cells, while $CD11c^+$$MHC\text{-}II^+$ cells further classified as moDCs. cDCs were defined as Gr-$1^-$$CD115^-$$CD11c^+$$MHC\text{-}II^+$ cells. (Figure S1A)

Figure 1A & B and Supplementary Fig. 1B depict the proportions of monocytes, moDCs and cDCs at different time points (Fig. 1A) with or without PA eye drop treatment (Fig. 1B). In the control group, monocytes and moDCs were detected at 7 dpi. The monocyte population increased from 7 to 10 dpi, followed by a sharp decrease from 10 to 16 dpi. The moDC population increased from 7 to 13 dpi, subsequently declining by 16 dpi. cDCs were detected after moDCs and remained relatively stable until 16 dpi. Upon administration of PA eye drop, the infiltration of monocytes and moDCs exhibited delayed detection, observed at 10 dpi. By 13 dpi, the treatment group mirrored the trends seen in the control group concerning monocyte counts, but displayed a substantial increase

by 16 dpi. The moDC population in the treatment group consistently declined from 10 dpi, preceding the control group's decline. However, no significant differences were observed between the control and treatment groups at any time point (Fig. 1C). Figure 1D illustrates the percentage of Gr-1$^+$CD115$^+$ CD11c$^+$MHC-II$^+$ cells relative to all Gr-1$^+$CD115$^+$ cells, reflecting the differentiation rate of moDCs. Both the control and treatment groups exhibited a sustained increase in differentiation rate from 7 to 13 dpi, peaking at 13 dpi, followed by a sharp decline at 16 dpi, with no significant difference between the groups. These findings indicated that PA did not inhibit moDC differentiation from monocyte. Furthermore, the number of moDCs was significantly higher than cDCs at 10, 13 and 16 dpi (Fig. 1E, $^*p<0.05$, $^{**}p<0.01$, $^{***}p<0.001$). These results indicating that following inflammation onset, monocytes swiftly responded, differentiating into DCs. PA administration did not impact the infiltration of moDCs or cDCs.

### MoDCs distributed predominantly at the superficial plexus of EAU retinal vessels

Immunofluorescence staining was performed to detect the distribution of moDCs within the retina by assessing the expression of the monocyte-derived cell marker CD115 and the DC marker CD209, both of which are expressed on the surface of moDC [25]. The retinal vasculature is organized into three plexuses: superficial, intermediate, and deep plexus (Schematic diagram in Fig. 2D). It was observed that moDCs were primarily distributed along the superficial plexus (Fig. 2A & B, Arrows; the positional mapping of each visual field is presented in Supplementary Fig. 2), with the minimal signal detected within the intermediate and deep plexuses (Figure S3). Quantification of the area displaying co-localized fluorescence signals in each visual field was performed to evaluate the abundance of moDCs within EAU retinas (Fig. 2C). Consistent with the flow cytometry outcomes, the results from fluorescence signal assessment showed a progressively ascending pattern in moDC infiltration, peaking at 13 dpi in the control group, but in the treatment group, the fluorescence signal peaked earlier, at 10 dpi, followed by a sustained decrease till 16 dpi.

### The expression of modc differentiation-associated cytokines in the early stages of EAU

Given the involvement of GM-CSF and TGF-β in monocyte differentiation and the synergistic effect of GM-CSF with IL-4 in stimulating both in vitro induction and maturation of moDCs from peripheral blood mononuclear cells [26, 27], the expression of GM-CSF and TGF-β1, the anti-inflammatory cytokines, *Il-10* and *Il-4*, as well as two transcription factors of moDCs, *Irf4* and *Zbtb46* were assessed in our research.

The western blotting results illustrated in Fig. 3A depict the expression levels of GM-CSF, TGF-β1, and β-actin (Full-length blots are presented in Supplementary Fig. 4). PA had no influence on the protein expression of GM-CSF at any time points (Fig. 3B). Whereas, a more pronounced inhibitory influence of PA was observed in the mRNA expression of GM-CSF (Fig. 4A, $^*p<0.05$, $^{**}p<0.01$, $^{****}p<0.0001$). On the other hand, GM-CSF expression exhibited no significant changes from 7 to 16 dpi in the absence of any prophylactic treatment, and the administration of PA led to a decrease in GM-CSF expression from 7 to 10 dpi. However, this suppressive effect was not sustained, as evidenced by a noticeable increase at 13 dpi (Fig. 3C, $^*p<0.05$, $^{**}p<0.01$).

Regarding TGF-β1, its protein expression was higher at 10 and 16 dpi with PA treatment (Fig. 3D, $^*p<0.05$, $^{**}p<0.01$). In the control group, TGF-β1 expression exhibited an apparent increase from 7 to 13 dpi (Fig. 3E, left, $^*p<0.05$, $^{**}p<0.01$). Under PA administration, TGF-β1 expression exhibited a more rapid rise from 7 to 10 dpi and maintained at the high level from 10 dpi to 16 dpi (Fig. 3E, $^{****}p<0.0001$). A similar trend was evident in the mRNA expression of *Tgf-b1*, displaying sustained elevation from 7 to 10 dpi with or without PA treatment, and PA significantly promoted the *Tgf-b1* mRNA expression from 7 to 16 dpi (Fig. 4B, $^{**}p<0.01$, $^{***}p<0.001$, $^{****}p<0.0001$).

Concerning the anti-inflammatory cytokines *Il-10* (Fig. 4C) and *Il-4* (Fig. 4D), their expressions declined under the influence of PA treatment at 7 and 10 dpi, respectively. Both cytokines exhibited a more significant increase at 16 dpi. During the early stage of EAU, both anti-inflammatory cytokines decreased initially from 7 to 13 dpi, followed by a sharp rise at 16 dpi. (Fig. 4C & D, $^*p<0.05$, $^{**}p<0.01$, $^{***}p<0.001$, $^{****}p<0.0001$)

In terms of the two transcription factors of moDCs, in the control group, PA exhibited minimal suppressive effects on the mRNA expression of *Irf4* until 16 dpi (Fig. 4E, $^{****}p<0.0001$). PA treatment advanced the elevation of *Zbtb46* mRNA expression to 13 dpi, a time point at which it remained unchanged in the control group until 16 dpi (Fig. 4F, $^*p<0.05$, $^{***}p<0.001$, $^{****}p<0.0001$).

## Discussion

After DCs capturing retina-associated autoantigens and activating CD4$^+$ T cells, CD4$^+$ T cells migrate to the eye and release matrix metalloproteinases (MMPs) and granzyme B, which disrupted the BRB and promoted the release of multiple inflammatory cytokines and chemokines, recruiting inflammatory cells including neutrophils and monocytes, thereby triggering a severe ocular autoimmune response [28]. Our research revealed that a notable infiltration of moDCs into the pathological retina during the early stage of EAU, detected earlier in higher

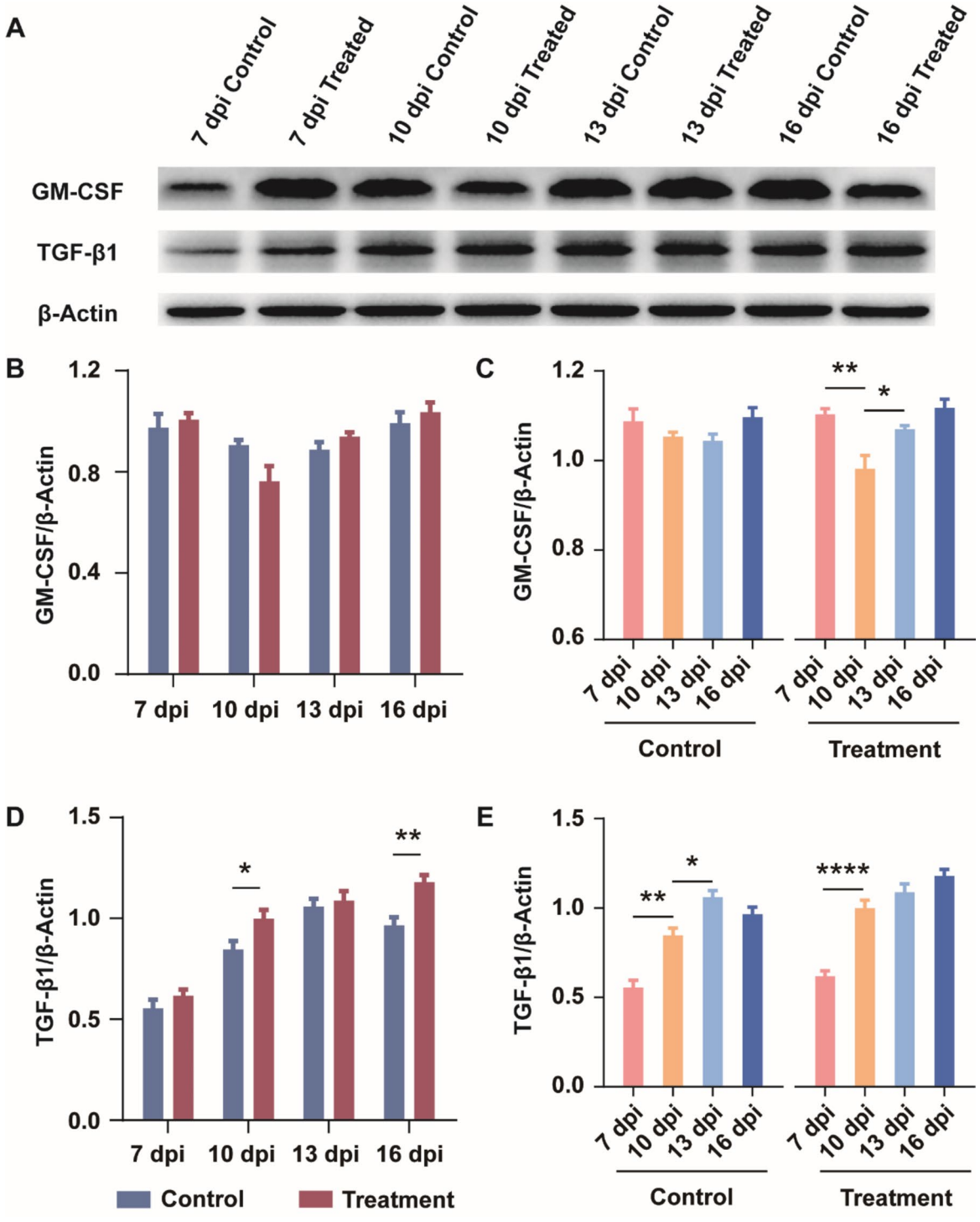


**Fig. 3** The expression of GM-CSF, TGF-β1 in retinas of EAU mice at different time points. (**A**) Western blot of the cropped blots showing protein expression in EAU retinas with or without PA treatment. (**B - E**) The relative quantity of GM-CSF (**B** & **C**) and TGF-β1 (**D** & **E**) expression with β-actin as a normalized loading. Note: The grouping of blots cropped from different gels. Full-length blots are presented in Supplementary Fig. 4 with the white dotted line showing the cropped position of images. The experiments were independently repeated three times with similar results. Data in **B** and **D** using unpaired t test, and data in **C** and **E** were compared using one-way ANOVA among multiple time points. ns, no significance. *$p < 0.05$, **$p < 0.01$, and ***$p < 0.001$, ****$p < 0.001$

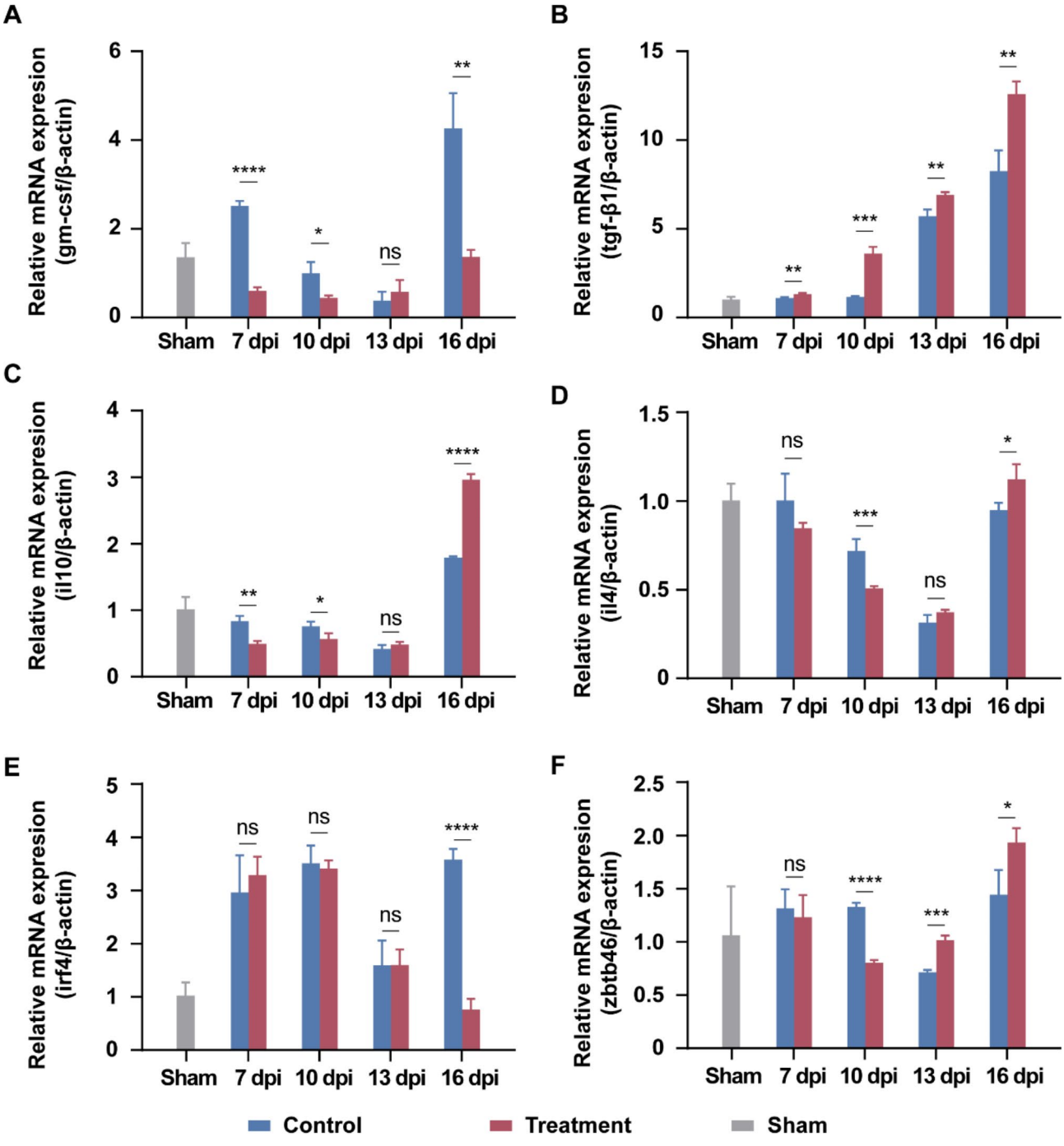


**Fig. 4** The mRNA expression of critical cytokines relative to the differentiation of moDCs. The mRNA expression of Gm-csf (**A**), Tgf-β1 (**B**), Il-10 (**C**), Il-4 (**D**), Irf4 (**E**) and Zbtb46 (**F**) of the retinas from EAU mice with or without PA treatment at different time points. The qRT-PCR values are normalized to β-actin. The experiments were independently repeated three times with similar results. *$p < 0.05$, **$p < 0.01$, and ***$p < 0.001$, ****$p < 0.001$

quantities compared to cDCs, which might be attributed to the abundance of critical cytokines that promote moDC differentiation from monocytes. Furthermore, the administration of PA eye drops exhibited limited efficacy in inhibiting the differentiation of moDCs.

Through whole-mount immunofluorescence staining of retina, we observed that moDCs are predominantly localized at the superficial layers of the retina. We speculated that this may be attributed to the invasive and infiltrative capabilities inherent of their monocytic precursors. Consequently, moDCs rapidly transmigrated through the vasculature within the uveal tract and infiltrate the whole layers of the retina, ultimately accumulating in the superficial retinal layers. Their specific

pathophysiological behaviors in EAU needs to be further investigated.

Both ocular and cerebral inflammation trigger the activation of microvascular endothelial cells and RPE cells [28], leading to increased adhesion molecule expression, facilitating the rapid recruitment of granulocytes followed by monocytes within a few hours [23]. Within sites of cerebral inflammation, various cells secrete GM-CSF and TGF-β, which have been shown to promote perivascular monocyte differentiation into moDCs [29]. moDCs exhibit different roles under diverse inflammatory environment, modulating the differentiation of naïve T cell into various subsets, including Th1 [30], Th2 [13] or Th17 cells [31], thereby initiating distinct T cell-mediated immune responses. Our results verified consistent GM-CSF protein expression and an upward trend in TGF-β1 protein and mRNA expression within EAU retinas. Taking into account the structural and physiological similarities between eyes and brain [32], our results suggest a potentially conducive microenvironment for moDC differentiation within the retina.

Following the onset of EAU, activation of retinal antigen-specific $CD4^+$ T cells triggers the production of matrix-degrading enzymes and metalloproteinases, disrupting the BRB and causing subsequent retinal antigen leakage [23]. Abundant DCs capture and present retinal auto-antigen in situ [7]. The absence of ocular lymphatic drainage limited the migration of cDCs, while monocytes have demonstrated the ability to differentiate into DCs at the inflammatory site. Our results highlight a more dynamic change in moDCs, as opposed to cDCs, during disease progression, indicating that upon crossing the BRB and infiltrating inflamed retinas, monocytes differentiate into moDCs, acting as the predominant DCs driving autoimmune reactions in early-stage EAU.

Corticosteroids serve as common first-line therapeutics for uveitis [33]. However, many individuals endure corticosteroid-refractory uveitis, with unknown underlying reasons [34]. In our research, we observed that the ocular administration of PA had no impact on the protein expression of GM-CSF. TGF-β1, known for its role in inflammation resolution [35], exhibited a persistent increase under the influence of PA. This elevation might contribute to the differentiation of moDCs, consequently promoting the autoimmune response in EAU.

Anti-inflammatory cytokines IL-10 and IL-4 play crucial roles, inhibiting the differentiation of naïve $CD4^+$ T cells into Th1 and Th17 cells [36] and suppressing IFN-γ secretion from Th1 cells [37]. IRF4 participate in myeloid DC differentiation and Th17 cell inductions [38], while ZBTB46 plays a role in suppressing *cd80/86* and *cd40* expression on DCs [39]. In our research, PA treatment failed to promote the expression of *Il-10*, *Il-4* and *Zbtb46* effectively during the early stage of EAU, exhibiting negligible influence on *Irf4* expression until 16 dpi, which indicating the conventional treatment minimally impacts EAU prognosis, emphasizing the imperative need for exploring novel therapeutics.

Besides, the synergistic action of TGF-β and IL-10 facilitates the differentiation of bone marrow-derived DCs (BMDCs) into regulatory DCs, which exhibited a diminished expression of CD80 and CD86, resulting in an impaired ability to activate T cells, thereby contributing to the amelioration of the course of EAU [40]. Our study did not detect a significant elevation in IL-10 levels throughout the course of EAU, irrespective of the administration of PA eye drop, which maybe another reason why PA eye drop contributing little to the remission of EAU. The precise influence of TGF-β1 and IL-10 on the maturation of moDCs as well as the effect of corticosteroids in this process needs further exploration.

Following the initiation of EAU, moDCs are predominantly numerical and exhibit dynamic alterations with disease progression in comparison to cDCs. This observation has led to the hypothesis that moDCs may play a pivotal role in the antigen presentation process during the early stage of EAU. However, the application of corticosteroid eye drops appears to have a minimal inhibitory effect on the differentiation of moDCs from monocytes and their subsequent infiltration into the retina. This could be a contributing factor to the limited efficacy observed with corticosteroid treatments in certain subtypes of uveitis. moDCs, a versatile and pivotal immune cell population, hold significant importance in the host's defence against infection and inflammation [41]. Despite their acknowledged significance, further investigation into moDCs' precise role in EAU is warranted. Our study proposes that early migration and infiltration of moDCs into the inflamed retina of EAU mice suggest modulating moDC activity might offer potential avenues for attenuating the autoimmune response, reducing inflammation, and reinstating immune homeostasis.

## Conclusion

In summary, we highlighted the substantial increase in both the quantity and differentiation rate of moDC during the early stages of EAU. These moDCs constituted the predominant infiltrating DC population within the pathological retina, surpassing cDCs under EAU conditions. The treatment of glucocorticoid eye drop exhibited minimal efficacy in suppressing the expression of ocular GM-CSF and TGF-β1, as well as in inhibiting the differentiation and infiltration of moDC. Therefore, we proposed moDCs rather than cDCs played a pivotal role in antigen presentation and supported the ocular autoimmune response. By understanding the in vivo distribution and functional significance of moDCs, it is possible to

develop novel therapies targeting inflammation-relative diseases.

**Abbreviations**

| | |
|---|---|
| ANOVA | Analysis of variance |
| APCs | Antigen-presenting cells |
| AU | Autoimmune uveitis |
| BBB | Blood-brain barrier |
| BMDCs | Bone-marrow derived dendritic cells |
| BRB | Blood-retina barrier |
| cDCs | Conventional dendritic cells |
| DCs | Dendritic cells |
| dpi | Days post-immunization |
| EAU | Experimental autoimmune uveitis |
| GM-CSF | Granulocyte-macrophage colony-stimulating factor |
| MHC | Histocompatibility complex |
| moDCs | Monocyte-derived dendritic cells |
| PA | Prednisolone acetate |
| PFA | Paraformaldehyde |
| PTX | Pertussis toxin |
| PVDF | Polyvinylidene difluoride |
| qRT-PCR | Quantitative real-time polymerase chain reaction |
| RIPA | Radio immunoprecipitation assay |
| RPE | Retinal pigment epithelial |
| SDS | Sodium dodecyl sulfate |
| SDS-PAGE | Sodium dodecyl sulfate - polyacrylamide gel electrophoresis |
| SEM | Standard error |
| TGF-β | Transforming growth factor beta |

## Supplementary Information

The online version contains supplementary material available at https://doi.org/10.1186/s12886-025-04014-x.

Supplementary Material 1

**Acknowledgements**
Not applicable.

**Author contributions**
XY is responsible for the conceptualization, methodology and validation. BY is responsible for the investigation and was the major contributor in writing the manuscript. YW is responsible for data curation, statistical analysis and manuscript edition. YC is responsible for the revision and statistical analysis of this manuscript. All authors read and approved the final manuscript.

**Funding**
This work was supported by National Natural Science Foundation of China under Grant 81970772; Tianjin Natural Science Foundation under Grant 21JCZDJC01250; Tianjin Key Medical Discipline (Specialty) Construction Project under Grant TJYXZDXK-016 A; Tianjin Health Research Project under Grant ZC20166; and Tianjin Eye Hospital Research Project under Grant YKYB1902.

**Data availability**
All data generated or analysed during this study are included in this published article and its supplementary information files.

## Declarations

**Ethics approval and consent to participate**
C57BL/6J mice were obtained from Beijing Vital River Laboratory Animal Technology Co., Ltd. (Beijing, China). Protocols for all animal procedures were approved by the Nankai University Animal Care and Use Committee and complied with National Institutes of Health (NIH) guidelines.

**Consent for publication**
Not applicable.

**Competing interests**
The authors declare no competing interests.

**Author details**
[1]School of Medicine, Nankai University, Tianjin, China
[2]Tianjin Eye Hospital, Tianjin, China
[3]Tianjin key Lab of Ophthalmology and Visual Science, Tianjin, China
[4]Aier Eye Hospital, Tianjin University, Tianjin, China

Received: 4 January 2024 / Accepted: 25 March 2025
Published online: 02 April 2025

**References**

1. Forrester JV, Kuffova L, Dick AD. Autoimmunity, autoinflammation, and infection in uveitis. Am J Ophthalmol. 2018;189:77–85.
2. Su Y, Tao T, Liu X, Su W. JAK-STAT signaling pathway in non-infectious uveitis. Biochem Pharmacol. 2022;204:115236.
3. Bonacini M, Soriano A, Cimino L, De Simone L, Bolletta E, Gozzi F, Muratore F, Nicastro M, Belloni L, Zerbini A, et al. Cytokine profiling in aqueous humor samples from patients with Non-Infectious uveitis associated with systemic inflammatory diseases. Front Immunol. 2020;11:358.
4. Nieto-Aristizabal I, Mera JJ, Giraldo JD, Lopez-Arevalo H, Tobon GJ. From ocular immune privilege to primary autoimmune diseases of the eye. Autoimmun Rev. 2022;21(8):103122.
5. Anderson DA 3rd, Dutertre CA, Ginhoux F, Murphy KM. Genetic models of human and mouse dendritic cell development and function. Nat Rev Immunol. 2021;21(2):101–15.
6. Heuss ND, Lehmann U, Norbury CC, McPherson SW, Gregerson DS. Local activation of dendritic cells alters the pathogenesis of autoimmune disease in the retina. J Immunol. 2012;188(3):1191–200.
7. Coillard A, Segura E. Antigen presentation by mouse monocyte-derived cells: Re-evaluating the concept of monocyte-derived dendritic cells. Mol Immunol. 2021;135:165–9.
8. Coillard A, Segura E. In vivo Differentiation of Human Monocytes. *Front Immunol* 2019, 10:1907.
9. Prevosto C, Goodall JC, Hill Gaston JS. Cytokine secretion by pathogen recognition receptor-stimulated dendritic cells in rheumatoid arthritis and ankylosing spondylitis. J Rheumatol. 2012;39(10):1918–28.
10. De Laere M, Berneman ZN, Cools N. To the brain and back: migratory paths of dendritic cells in multiple sclerosis. J Neuropathol Exp Neurol. 2018;77(3):178–92.
11. Ludewig P, Gallizioli M, Urra X, Behr S, Brait VH, Gelderblom M, Magnus T, Planas AM. Dendritic cells in brain diseases. Biochim Biophys Acta. 2016;1862(3):352–67.
12. Parikh SV, Malvar A, Shapiro J, Turman JM, Song H, Alberton V, Lococo B, Mejia-Vilet JM, Madhavan S, Zhang J, et al. A novel inflammatory dendritic cell that is abundant and contiguous to T cells in the kidneys of patients with lupus nephritis. Front Immunol. 2021;12:621039.
13. Eguiluz-Gracia I, Bosco A, Dollner R, Melum GR, Lexberg MH, Jones AC, Dheyauldeen SA, Holt PG, Baekkevold ES, Jahnsen FL. Rapid recruitment of CD14(+) monocytes in experimentally induced allergic rhinitis in human subjects. J Allergy Clin Immunol. 2016;137(6):1872–e18811812.
14. Liu M, Liu F, Pan Y, Xiong Y, Zeng X, Zheng L, Zhao H, Li Y, Liu D. Oxymatrine ameliorated experimental colitis via mechanisms involving inflammatory DCs, gut microbiota and TLR/NF-kappaB pathway. Int Immunopharmacol. 2023;115:109612.
15. Hussain A, Rafeeq H, Munir N, Jabeen Z, Afsheen N, Rehman KU, Bilal M, Iqbal HMN. Dendritic Cell-Targeted therapies to treat neurological disorders. Mol Neurobiol. 2022;59(1):603–19.
16. Segura E, Touzot M, Bohineust A, Cappuccio A, Chiocchia G, Hosmalin A, Dalod M, Soumelis V, Amigorena S. Human inflammatory dendritic cells induce Th17 cell differentiation. Immunity. 2013;38(2):336–48.
17. Tang-Huau TL, Segura E. Human in vivo-differentiated monocyte-derived dendritic cells. Semin Cell Dev Biol. 2019;86:44–9.
18. Marzaioli V, Canavan M, Floudas A, Flynn K, Mullan R, Veale DJ, Fearon U. CD209/CD14(+) dendritic cells characterization in rheumatoid and psoriatic arthritis patients: activation, synovial infiltration, and therapeutic targeting. Front Immunol. 2021;12:722349.
19. Inomata H, Rao NA. Depigmented atrophic lesions in sunset glow fundi of Vogt-Koyanagi-Harada disease. Am J Ophthalmol. 2001;131(5):607–14.

20. Bascuas T, Zedira H, Kropp M, Harmening N, Asrih M, Prat-Souteyrand C, Tian S, Thumann G. Human retinal pigment epithelial cells overexpressing the neuroprotective proteins PEDF and GM-CSF to treat degeneration of the neural retina. Curr Gene Ther. 2022;22(2):168–83.
21. Mattapallil MJ, Silver PB, Cortes LM, St Leger AJ, Jittayasothorn Y, Kielczewski JL, Moon JJ, Chan CC, Caspi RR. Characterization of a new epitope of IRBP that induces moderate to severe uveoretinitis in mice with H-2b haplotype. Invest Ophthalmol Vis Sci. 2015;56(9):5439–49.
22. Chen Y, Chen Z, Chong WP, Wu S, Wang W, Zhou H, Chen J. Comparative analysis of the interphotoreceptor retinoid binding proteininduced models of experimental autoimmune uveitis in B10.RIII versus C57BL/6 mice. Curr Mol Med. 2018;18(9):602–11.
23. Li J, Chu W-K. An experimental autoimmune uveoretinitis model and intraocular inflammation. Hong Kong J Ophthalmol [Internet]. 2016;20(1):7–17.
24. Chan CC, Caspi RR, Ni M, Leake WC, Wiggert B, Chader GJ, Nussenblatt RB. Pathology of experimental autoimmune uveoretinitis in mice. J Autoimmun. 1990;3(3):247–55.
25. Martinez-Carmona M, Lucas-Ruiz F, Gallego-Ortega A, Galindo-Romero C, Norte-Munoz M, Gonzalez-Riquelme MJ, Valiente-Soriano FJ, Vidal-Sanz M, Agudo-Barriuso M. Ly6c as a new marker of mouse blood vessels: qualitative and quantitative analyses on intact and ischemic retinas. Int J Mol Sci 2021, 23(1).
26. Denniston AK, Tomlins P, Williams GP, Kottoor S, Khan I, Oswal K, Salmon M, Wallace GR, Rauz S, Murray PI, et al. Aqueous humor suppression of dendritic cell function helps maintain immune regulation in the eye during human uveitis. Invest Ophthalmol Vis Sci. 2012;53(2):888–96.
27. Schreurs MWJ, Eggert AAO, de Boer AJ, Figdor CG, Adema GJ. Generation and functional characterization of mouse monocyte-derived dendritic cells. Eur J Immunol. 1999;29(9):2835–41.
28. Egwuagu CE, Alhakeem SA, Mbanefo EC. Uveitis: molecular pathogenesis and emerging therapies. Front Immunol. 2021;12:623725.
29. Ifergan I, Kebir H, Bernard M, Wosik K, Dodelet-Devillers A, Cayrol R, Arbour N, Prat A. The blood-brain barrier induces differentiation of migrating monocytes into Th17-polarizing dendritic cells. Brain. 2008;131(Pt 3):785–99.
30. Gu FF, Wu JJ, Liu YY, Hu Y, Liang JY, Zhang K, Li M, Wang Y, Zhang YA, Liu L. Human inflammatory dendritic cells in malignant pleural effusions induce Th1 cell differentiation. Cancer Immunol Immunother. 2020;69(5):779–88.
31. Reynolds G, Gibbon JR, Pratt AG, Wood MJ, Coady D, Raftery G, Lorenzi AR, Gray A, Filer A, Buckley CD, et al. Synovial CD4 + T-cell-derived GM-CSF supports the differentiation of an inflammatory dendritic cell population in rheumatoid arthritis. Ann Rheum Dis. 2016;75(5):899–907.
32. Waithe OLY, Muthusamy S, Anderson A, Hein T, Childs E, Tharakan B. Homocysteine-induced barrier dysfunction and hyperpermeability in the Blood-Brain and Blood-Retinal barrier: role of NLRP3 inflammasome pathway. Physiology. 2023;38(S1):5734669.
33. Merrill P, Pavesio C, Banker AS. Emerging treatments for Non-infectious uveitis. US Ophthalmic Rev 2018, 11(2).
34. Chen TS, Tsang WM, Enkh-Amgalan I, Hwang YS. Mycophenolate sodium in the treatment of corticosteroid-refractory non-infectious inflammatory uveitis (MySTRI study). Eye (Lond). 2020;34(11):2098–105.
35. Ohta K, Wiggert B, Yamagami S, Taylor AW, Streilein JW. Analysis of Immunomodulatory activities of aqueous humor from eyes of mice with experimental autoimmune uveitis. J Immunol. 2000;164(3):1185–92.
36. Fan W, Wang X, Zeng S, Li N, Wang G, Li R, He S, Li W, Huang J, Li X, et al. Global lactylome reveals lactylation-dependent mechanisms underlying T(H)17 differentiation in experimental autoimmune uveitis. Sci Adv. 2023;9(42):eadh4655.
37. Weinstein JE, Pepple KL. Cytokines in uveitis. Curr Opin Ophthalmol. 2018;29(3):267–74.
38. Chen J, Martindale JL, Abdelmohsen K, Kumar G, Fortina PM, Gorospe M, Rostami A, Yu S. RNA-Binding protein HuR promotes Th17 cell differentiation and can be targeted to reduce autoimmune neuroinflammation. J Immunol. 2020;204(8):2076–87.
39. Shao T, Ji JF, Zheng JY, Li C, Zhu LY, Fan DD, Lin AF, Xiang LX, Shao JZ. Zbtb46 controls dendritic cell activation by reprogramming epigenetic regulation of cd80/86 and cd40 costimulatory signals in a zebrafish model. J Immunol. 2022;208(12):2686–701.
40. Usui Y, Takeuchi M, Hattori T, Okunuki Y, Nagasawa K, Kezuka T, Okumura K, Yagita H, Akiba H, Goto H. Suppression of experimental autoimmune uveoretinitis by regulatory dendritic cells in mice. Archives Ophthalmol (Chicago Ill: 1960). 2009;127(4):514–9.
41. Hubert M, Gobbini E, Bendriss-Vermare N, Caux C, Valladeau-Guilemond J. Human Tumor-Infiltrating dendritic cells: from in situ visualization to High-Dimensional analyses. Cancers (Basel) 2019, 11(8).


## Publisher's note